Synthesis of Epoxy–Montmorillonite Nanocomposite

K. H. Chen, S. M. Yang

Department of Chemical Engineering, National Central University, Chung-Li, Taiwan 320, Republic of China

Received 30 May 2001; accepted 19 December 2001

ABSTRACT: To synthesize an epoxy–montmorillonite nanocomposite, the intercalation of clay layers with acid onium ions {$[H_3N(CH_2)_{n-1}COOH]^+$, $[H_3N(CH_2)_{n-1}CH_3]^+$, $[H_3N(CH_2)\_NH_2]^+$, and $[H_3N(CH_2)_nNH_3]^{2+}$} by different methods were studied. The intercalated clay was characterized by XRD, ICP, and CHN elemental analysis. An acid onium ion $[H_3N(CH_2)_{17}CH_3]^+$ enlarged the *d*-spacing of CWC–, AMS–, and Kunipia–montmorillonite to 21.6, 18.1, and 20.7 Å, respectively. The results of CHN elemental analysis confirmed that onium ions were intercalated between the clay layers. Ion exchange of montmorillonite with onium ions is a better way to intercalate more onium ions. Among those onium ions mentioned above, $[H_3N(CH_2)_nNH_3]^{2+}$ displaced more sodium ions from the clay layers than did the others. An epoxy–montmorillonite nanocomposite was synthesized by heating a mixture of $[H_3N(CH_2)_{17}CH_3]^+$–montmorillonite (CWC) with an epoxy monomer and curing agent. The nanocomposite was characterized by XRD, TEM, DSC, UV, TGA, and Instron testing. TEM photographs showed that the spacing between the clay layers was further enlarged to about 50 Å and no segregation between the clay particle and the polymer was observed. The glass transition temperature of the nanocomposite containing 20 phr of $[H_3N(CH_2)_{17}CH_3]^+$–montmorillonite (CWC) increased from 108.4 to 146.1°C. Especially, the nanocomposite possesses higher water resistance than that of the epoxy resin or of the physical mixture of epoxy and montmorillonite (CWC). According to the transmittance measurement (λ = 550 nm), the nanocomposite shows good light transmittance. Although, we cannot improve the mechanical properties, improvements of other properties can be evidenced for the formation of nanoscale composites. © 2002 Wiley Periodicals, Inc. J Appl Polym Sci 86: 414–421, 2002

Key words: glass transition; nanocomposites; polyethers; TEM

INTRODUCTION

Clay or other inorganic materials have been added into polymers as fillers to improve the mechanical properties of the polymer. Because of the interfacial interaction between a polymer and clay, the nanocomposite leads to improved properties when compared to micro- and macrocomposites. The improvements of the properties of composites are affected by the exfoliation of the clay in the polymer matrix. The potential improvements include water resistance, flame retardation, and gas permeability. So, it is primary work to understand the exfoliation of the clay in the polymer. Recently, a nanocomposite of a clay–polymer was formed by intercalation of clay with organic ions, followed by polymerization of the polymer precursor inside the clay layers. Faguy et al. polymerized pyrrole within montmorillonite.[1] The composite showed properties of both the conducting polymer and the host material. Toyota researchers polymerized nylon-6 in the presence of delaminated $[H_3N(CH_2)_{11}COOH]^+$–montmorillonite.[2,3] Highly dispersed clay layers in the nylon–6 matrix greatly improved the tensile strength, tensile modulus, and heat-distortion temperature. Other polymer–clay composites, such as polystyrene,[4] epoxy resin,[5–7] poly(ethylene oxide),[8–10] polyimide,[11] and polycaprolactone[12] were also reported.

Epoxy resin is often used in integrated circuit (IC) packaging and printed circuit boards (PCBs), such as in pin grid array packaging, ball grid array packaging, and multichip modules. To improve the thermal properties and mechanical properties, inorganic material such as clay is also used as additives in epoxy resin. The synthesis of epoxy–clay nanocomposites were reported previously.[13–15] Wang et al. studied a newly developed class of paraffinlike organomagadiite intercalates. The epoxy–magadiite nanocomposite is more optically transparent than is the epoxy–smectite nanocomposite.[16,17] Vaia et al. provided a new experimental insight into the interlayer and phase state of intercalated alkylammonium silicates by FTIR and XRD.[18] By monitoring frequency shifts of the asymmetric CH_2 stretching and bending vibrations with FTIR, they found that the intercalated chains exist in states with varying degrees of order. Chen and Wu added china clay ($3Al_2O_3 \cdot 2SiO_2$) to the epoxy matrix and the results show that the influence of the boundary layer is important and that it can influence the density. The Young's modulus and tensile strength of the composite can be estimated from the component phases.[19] Lee intercalated the epoxy polymer into the interlayer of Na^+–montmorillonite by a step type of polymeriza-

Correspondence to: S. M. Yang (smyang@cc.ncu.edu.tw).

Journal of Applied Polymer Science, Vol. 86, 414–421 (2002)

tion in an aqueous emulsion media; the acetone-extracted products show that the basal spacing of the montmorillonite is expanded from 0.96 to 1.64 nm.[20] Lee and Lichtenhan investigated thermal and viscoelastic property enhancement on crosslinked epoxy using two types of nanoreinforcement, namely, organoion-exchange clay and polymerizable polyhedral oligomeric silsesquioxane macromers; however, for an epoxy network reinforced with clay, the results showed no effect on the T_g due to the presence of clay reinforcements.[21] Although considerable research has been reported on the synthesis of nanocomposites, most reports focused on the modification of clay by ion exchange and the properties of the composite. Hence, the delamination of montmorillonite by different methods, clays, and onium ions were studied in this report. The epoxy–montmorillonite nanocomposites were characterized by XRD, TEM, DSC, UV, TGA, and Instron testing. Besides, due to the applications of nanocomposites, properties such as heat resistance, water resistance, tensile strength, and optical properties are also reported.

EXPERIMENTAL

Materials

Na^+–montmorillonite with an exchange capacity of 145 mequiv/100 g (CWC) and 125 mequiv/100 g (AMS) were obtained from Nanocor Inc (Chicago, IL). Na^+–montmorillonite with an exchange capacity of 125 mequiv/100 g (Kunipia-F) was donated by the Kunimine Industrial Co (Chiyoda-ku, Japan). Diglycidyl ether of bisphenol A (DGEBA, epoxide equivalent weight 178, DER332) was obtained from Dow Chemicals (Midland, MI). Nadic methyl anhydride (NMA, GR), benzyldimethylamine (BDMA, 98%), alkylamines [$CH_3(CH_2)_{n-1}NH_2$, 99% for $n = 6$, 98% for $n = 12$, and 97% for $n = 18$], aminocarboxylic acids [$H_2N(CH_2)_{n-1}COOH$, 99% for $n = 6$ and 98% for $n = 12$], and diamines [$H_2N(CH_2)_nNH_2$, 98% for $n = 6$ and 99% for $n = 12$] were obtained from Aldrich (St. Louis, MO) and used as received.

Intercalation of clay with organic onium ions

The protonated forms of amine were formed by dissolving 5 mmol of the free amine in 500 mL of a 0.01*N* (0.02*N* for diamine) aqueous HCl solution at 60°C. Five grams of clay was thoroughly dispersed in the onium ion solution at 60°C for 3 h. The cation-exchanged montmorillonite was separated by centrifugation and washed with deionized water. The procedure was repeated until no white precipitate of AgCl was observed when a drop of 0.1*N* $AgNO_3$ was added to the centrifugate.

Intercalation by acid–base reactions was carried out in the vapor phase and an aqueous solution. A sodium form of montmorillonite was converted into acidic form by ion exchange with an aqueous HCl (1*M*) solution. In the vapor-phase reaction, dodecylamine was heated at 140°C, the vapor of dodecylamine [$H_2N(CH_2)_{11}CH_3$] was passed by H^+–montmorillonite for 4 h, and then montmorillonite was sealed with vapor overnight. In an aqueous solution reaction, 5 g of H^+–montmorillonite was thoroughly dispersed in the dodecylamine solution (0.01*M*) at 60°C for 3 h.

Synthesis of epoxy–montmorillonite nanocomposite

Intercalated clay was added with stirring to DGEBA (DER 332) and cured by addition of NMA and BDMA. The amount of the curing agent used for each formulation was as follows: 87.5 phr (per hundred resin) of NMA and 5 phr of BDMA. The clay/DGEBA mixtures were heated at 70°C with stirring for 10 min and then sonicated for 30 min at 70°C using an ultrasonic cleaner. Following sonication, samples were heated at 70°C for 1 h and the curing agent was added with thorough mixing and then dispensed into Teflon molds or beakers. All samples were cured at 80°C for 1 h, 100°C for 1 h, 120°C for 1 h, 150°C for 6 h, and 200°C for 1 h.

Characterization

X-ray diffraction (XRD) experiments were performed on a Siemens D-500 X-ray diffractometer with CuKα as a radiation source, operated at 40 kV and 30 mA. The polymerization temperature and T_g were determined by a Perkin–Elmer DSC7 under N_2 (50 mL/min) with a heating rate of 20°C/min. Indium and zinc were used as calibration standards.

The amount of the sodium ion exchanged was determined by a JOBIN YVON JY-24 ICP/AES. TEM photographs were taken with a JEOL JEM2000 FX II using an accelerating voltage of 160 kV. The sample was ultrathin-sectioned (75-nm-thick slices) using a microtome equipped with a glass knife. TGA analyses were carried out under N_2 on a Perkin–Elmer TGA7 thermogravimetric analyzer at a heating rate of 10°C/min. A sample mechanical measurement was performed at ambient temperature according to ASTM procedure D638-64T using a United Testing System. Tensile testing was obtained with a Instron Model 4302 using a strain rate of 1 mm/min. The volume of the samples for water-content measurements were 15 $\times$ 15 $\times$ 3 mm. The samples were placed in an oven at 110°C for 24 h, then immersed in water at 23°C for 24 h. The water content of the sample is calculated by the formula

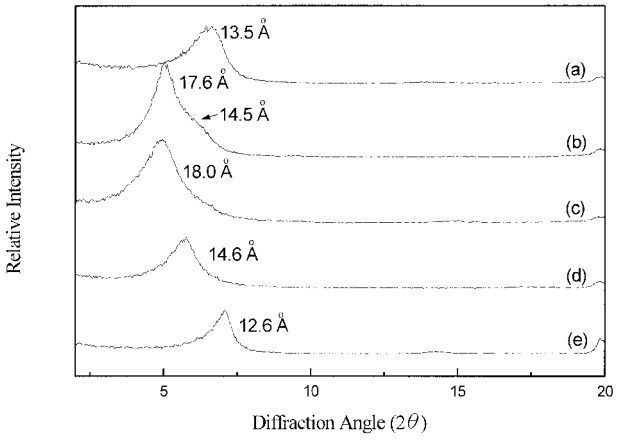

Figure 1 XRD patterns of $[H_3N(CH_2)_{11}CH_3]^+$–montmorillonite (CWC) hybrids prepared by (a) an acid–base method by vapor, (b) an acid–base method by aqueous medium, and (c) an ion-exchanged method and (d) H^+–montmorillonite (CWC) and (e) pristine Na^+–montmorillonite (CWC).

$$\frac{\text{weight}_{23^\circ\text{C,24h in water}} - \text{weight}_{110^\circ\text{C,24h in oven}}}{\text{weight}_{110^\circ\text{C,24h in oven}}} \times 100\%$$

RESULTS AND DISCUSSION

Intercalation of montmorillonite

Ion exchange of Na^+ gallery cations in the pristine mineral by onium ions allows modification of the layer surface for intercalation of epoxy monomers. To exfoliate the clay layers, Na^+ must be completely exchanged, because unexchanged Na^+ centers in alkylammonium-exchanged clays may act as pinning points to prevent gallery expansion by the polymer precursors.[22] Furthermore, the dielectric constant of the product may be affected by the residual Na^+ or other metal ions. According to our study, the amount of Na^+ ions displaced reached a plateau when montmorillonite was exchanged with onium ions at 60°C for 3 h. The same amount of displaced Na^+ was found at higher temperature. It is noteworthy that the *d*-spacing of the exchanged clay at 35°C for 3 h also reached 16.4 Å. The solubility of alkylammonium in water decreases with increasing alkyl chain length. It is necessary to keep the temperature at 60°C for higher solubility of the long-chain alkylammonium ion in water. The result of ICP analyses shows that no more Na^+ ions were further displaced by exchanging the clay twice with $[NH_3(CH_2)_{11}CH_3]^+$. To achieve the maximum amount of exchanged alkylammonium ions, we studied the effect of the intercalating methods, clays, and onium ions on the intercalation of montmorillonite.

Effect of intercalating methods

Figure 1 shows the XRD pattern of onium ions intercalated, H^+– and Na^+–montmorillonites (CWC). The spacings of intercalated clay formed from an acid–base reaction in the vapor phase, an acid–base reaction in an aqueous solution, and ion exchange of Na^+–montmorillonite are 13.5, 17.6, and 18.0 Å, respectively. A shoulder corresponding to the *d* spacing of 14.5 Å appears in the XRD pattern of montmorillonite intercalated by an acid–base reaction in an aqueous solution. The peak occurs at the same diffraction angle as that of a 0.15*M* HCl aqueous solution-exchanged clay. We assigned the *d*-spacing of this shoulder peak to the hydronium ion intercalated clay. The XRD pattern of (b) reveals that only part of the clay was intercalated by onium ions. Table I shows the *d*-spacing and the amount of amine for montmorillonite (CWC) intercalated by different methods. Elemental analysis of CHN also showed that a higher level of intercalation occurs in clay intercalated by the ion-exchange method. The amount of onium ions intercalated in the clay layers are 407.5, 617.6, and 1184 μmol/g clay by an acid–base reaction in the vapor phase, an acid–base reaction in an aqueous solution, and an ion-exchange reaction, respectively. The results indicate that an acid–base reaction in the vapor phase is not an effective method to enlarge the *d*-spacing between clay layers.

Effect of clay with different interlayer charge density

The cation-exchanged capacity (CEC) is a useful parameter for interlayer charge density. Figure 2 shows

TABLE I
Amount of Amine Intercalated in Montmorillonite (CWC) and *d*-Spacing of Intercalated Montmorillonite by Different Method

	$[NH_3(CH_2)_{11}CH_3]^+$–montmorillonite	
Method of intercalation	*d*-Spacing (Å)	Amount of amine[a] (μmol/g clay)
Acid–base intercalation in vapor	13.5	407.5
Acid–base intercalation in aqueous medium	17.6	617.6
Ion-exchanged intercalation	18.0	1184.4

[a] Determined by CHN elemental analysis.

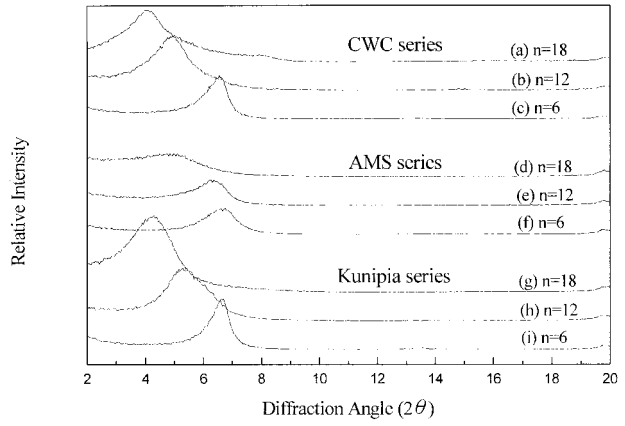

Figure 2 XRD patterns of various hybrids of CWC–montmorillonite, AMS–montmorillonite, and Kunipia–montmorillonite intercalated with $[H_3N(CH_2)_{n-1}CH_3]^+$.

XRD curves of intercalated clay of different chain lengths of $[NH_3(CH_2)_{n-1}CH_3]^+$ and clays from different sources. Table II summarizes the *d*-spacing of $[NH_3(CH_2{}_{n-1}CH_3]^+$–montmorillonite and the amount of Na^+ displaced by protonated alkyl amines. The order of decreasing *d*-spacing of the $[H_3^+N(CH_2)_{n-1}CH_3]^+$–montmorillonite ($n$ = 6, 12, and 18) are CWC > Kunipia > AMS, in accordance with the order of the amount of displaced sodium ions. The amount of alkylammonium ion that can be intercalated into the clay layer may depend on the interlayer charge density. Since the order of decreasing CEC values are CWC > AMS > Kunipia, we expect that the *d*-spacing of the $[H_3N(CH_2)_{n-1}CH_3]^+$–montmorillonite will be CWC > AMS > Kunipia. The result is not the same as we expected. There will be some other factors influencing the *d*-spacing of the intercalated clay. The hydrophobicity, interfacial interaction, and other properties of the montmorillonite may play important roles.

Effect of onium ions

In this section, montmorillonite (CWC) intercalated by various cations was studied. The cations intercalated were $[H_3N(CH_2)_{n-1}CH_3]^+$ (n = 6, 12, and 18), $[H_3N(CH_2)_{n-1}COOH]^+$ (n = 6, 12), $[H_3N(CH_2)_nNH_2]^+$ (n = 6, 12), and $[H_3N(CH_2)_nNH_3]^{2+}$ (n = 6, 12). Due to differences in the chain length, functional groups, and charge density of the exchange cations, the *d*-spacing differs for the hybrids. In Table III are listed the results of the XRD and elemental analysis of montmorillonite (CWC) intercalated with various cations. The effects of various factors are discussed below:

Effect of chain length

As shown by the data in Table III, we find that *d*-spacing of intercalated clay increases with the chain length when the intercalated onium ions are $[H_3N(CH_2{}_{n-1}CH_3]^+$ and $[H_3N(CH_2)_{n-1}COOH]^+$. The results agree with previous reports.[5] In Table III, the amount of gallery cations all increase from n = 6–12. In general, as the chain length increases, the intercalated chains adopt a more ordered, liquidlike structure, resulting from a decrease in the *gauche/trans* conformer ratio.[18] The ordered form will have a larger packing capacity than that of the disordered form. These results may also indicate that the onium ions' aggregation in the interlayer was changed from monolayers to bilayers. The increase in gallery height is accompanied by a decreasing amount of gallery cations when the n of $[H_3N(CH_2)_{n-1}CH_3]^+$ changes from 12 to 18. Since with a longer chain length the the alkylamines are more hydrophobic, the solubility of alkylamines (>0.01*M* for $n \leq 12$ and about 0.004*M* for n = 18 at 60°C) in an aqueous solution decrease with an increasing chain length. For the above reason, $[H_3N(CH_2)_{17}CH_3]^+$–montmorillonite has a smaller amount of gallery cations. Our study also evidenced (not showed here) that there was a correlation between the onium ion concentration (0.004–0.0001*M*) of the bulk solution and the amount of intercalated gallery cations within the clay layers. Another reason for a smaller amount of gallery cations in $[H_3N(CH_2)_{17}CH_3]^+$–montmorillonite is that the limited interlayer spacing can only accommodate fewer long-chain onium ions. The concentration of onium

TABLE II
***d*-Spacing of the Hybrids and the Amount of Na^+ Displaced by Protonated Alkyl Amines**

	CWC		AMS		Kunipia	
Gallery cation	*d*-Space (Å)	Exchanged Na^+[a]	*d*-Space (Å)	Exchanged Na^+[a]	*d*-Space (Å)	Exchanged Na^+[a]
Na^+	12.6	—	12.8	—	12.8	—
$[NH_3(CH_2)_5CH_3]^+$	13.5	725.5	13.3	667.1	13.3	681.2
$[NH_3(CH_2)_{11}CH_3]^+$	18.0	1013.5	14.0	803.6	16.7	821.6
$[NH_3(CH_2)_{17}CH_3]^+$	21.6	948.9	18.1	827.7	20.8	743.5

The CEC of CWC–montmorillonite, AMS–montmorillonite, and Kunipia–montmorillonite are 1450, 1250, and 1150 μmol/g clay, respectively.

[a] The unit of the exchanged Na^+ was μmol/g clay.

TABLE III
Summary of XRD, ICP, and CHN Data for Various Hybrids

	CWC–montmorillonite (1450 μmol/g clay)			
		Na^+		
Gallery cation	*d*-Space (Å)	Displaced Na^+ (μmol/g clay)	Displaced percentage (%)	Amount of gallery cation (μmol/g clay)
Na^+ (pristine clay)	12.6	—	—	1434.8
$[H_3N(CH_2)_5CH_3]^+$	13.5	725.5	50.0	745.3
$[H_3N(CH_2)_{11}CH_3]^+$	18.0	1013.5	69.9	1184.4
$[H_3N(CH_2)_{17}CH_3]^+$	21.6	948.9	65.4	770.8
$[H_3N(CH_2)_5COOH]^+$	13.1	687.0	47.4	419.4
$[H_3N(CH_2)_{11}COOH]^+$	17.8	889.2	61.3	735.7
$[H_3N(CH_2)_6NH_2]^+$	13.1	1241.7	85.6	574.9
$[H_3N(CH_2)_{12}NH_2]^+$	13.8	1209.8	83.4	754.9
$[H_3N(CH_2)_6NH_3]^{2+}$	13.0	1290.4	89.0	513.3
$[H_3N(CH_2)_{12}NH_3]^{2+}$	13.7	1220.1	84.1	558.8

ions also has a significant effect on the *d*-spacing of intercalated clay. When the onium ion concentration of the bulk solution was lower than 0.0025*M*, it was difficult to enlarge the interlayer spacing of the clay.

Effect of functional group

Depending on the *d*-spacing and the chain length, the $[H_3N(CH_2)_{11}CH_3]^+$ and $[H_3N(CH_2)_{11}COOH]^+$ chains are thought to lie as a bilayer. Also, the $[H_3N(CH_2)_5CH_3]^+$, $[H_3N(CH_2)_{11}COOH]^+$, $[H_3N(CH_2)_nNH_2]^+$, and $[H_3N(CH_2)_nNH_3]^{2+}$ ($n = 6$ and 12) chains all lie as a lateral monolayer. Finally, the $[H_3N(CH_2)_{11}CH_3]^+$ was expected to lie pseudo-trimolecular.[13,23] The interactions occurring at the onium ion–clay surface are very complex. The attractive interactions are different for different functional groups. In accordance of the relative small *d*-spacing and high displaced percentage of diamines (13.1–13.8 Å and 83.4–85.6%), we are sure that the diamines have the largest interaction between onium ions and the clay surface. In this study, the order of interaction between onium ions and the clay surface are $[H_3N(CH_2)_nNH_3]^{2+} > [H_3N(CH_2)_{n-1}CH_3]^+ > [H_3N(CH_2)_{n-1}COOH]^+$, in accordance with the amount of gallery cations.

Effect of charge density

The dependence of *d*-spacing on the charge density was also investigated. Table III compares $[H_3N(CH_2)_nNH_3]^{2+}$ and $[H_3N(CH_2)_nNH_2]^+$ hybrids of different charge density, but similar chain length. As the charge density increases, *d*-spacing decreases from 13.1 to 13.0 Å for $n = 6$ and from 13.8 to 13.7 Å for $n = 12$. Although the difference in *d*-spacing is not so clear, it also shows us some evidence that $[H_3N(CH_2)_nNH_3]^{2+}$ has a stronger affinity with the layers of clay on both sides than that of $[H_3N(CH_2)_nNH_2]^+$. Thus, it is harder for $[H_3N(CH_2)_nNH_3]^{2+}$ to increase the *d*-spacing. It is noteworthy that, because the amount of gallery cations that can be loaded into the galleries of clay is dependent on the charge density of the onium ion, the amount of $H_2N(CH_2)_nNH_2$ in CWC–montmorillonite also depends on the charge density of the onium ion. Thus, the amount of gallery cations decreased from 574.9 μmol/g clay for $[H_3N(CH_2)_5NH_2]^+$ to 513.3 μmol/g clay for $[H_3N(CH_2)_5NH_3]^{2+}$ and from 754.9 μmol/g clay for $[H_3N(CH_2)_{11}NH_2]^+$ to 558.8 μmol/g clay for $[H_3N(CH_2)_{11}NH_3]^{2+}$. Because of the difference in the *d*-spacing, displaced percentage, and amount of gallery is not very distinguished, it may be indicated that $[H_3N(CH_2)_nNH_2]^+$ and $[H_3N(CH_2)_nNH_3]^{2+}$ are formed at the same time for 0.01*M* $H_2N(CH_2)_{11}NH_2$ dissolving in 0.01*M* HCl. So, it is possible for the designed $[H_3N(CH_2)_nNH_2]^+$–montmorillonite to coexist with $[H_3N(CH_2)_nNH_3]^{2+}$–montmorillonite. The $[H_3N(CH_2)_nNH_2]^+$–montmorillonite really caused the designed $[H_3N(CH_2)_nNH_2]^+$–montmorillonite to have a smaller amount of gallery cations and bigger *d*-spacing than those of $[H_3N(CH_2)_nNH_3]^{2+}$–montmorillonite.

In this study, the maximum *d*-spacing of 21.6 Å was observed for $[H_3N(CH_2)_{17}CH_3]^+$–montmorillonite (CWC). A large amount of epoxy monomer can be loaded into clay galleries with large interlayer spacing. So, we chose $[H_3N(CH_2)_{17}CH_3]^+$–montmorillonite (CWC) for the synthesis of the clay–epoxy nanocomposite.

Synthesis of the nanocomposite

To verify the degree of swelling of $[H_3N(CH_2)_{17}CH_3]^+$–montmorillonite (CWC) by epoxy monomers, XRD patterns of the swelled clay were studied. The results shown in Figure 3 indicate that the *d*-spacing of intercalated clay increased further in contact with the epoxy monomer even at room temperature. After curing at elevated temperature (200°C), the *d*-spacing is too large to be ob-

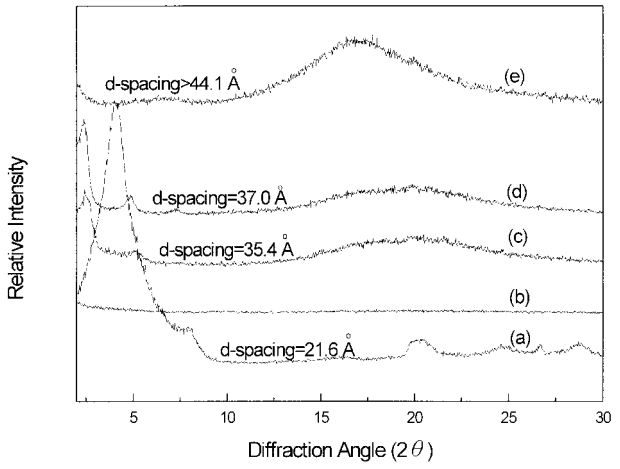

Figure 3 XRD patterns of (a) $[H_3N(CH_2)_{17}CH_3]^+$–montmorillonite (CWC), (b) DER 332 epoxy, (c) mixing $[H_3N(CH_2)_{17}CH_3]^+$–montmorillonite (CWC) with 20 phr and DER 332 epoxy, (d) of (c) heated at 105°C for 8 h, and (e) of (d) then cured at 150°C for 6 h and 200°C for 6 h.

served by XRD. The TEM photograph of the nanocomposite containing 20 phr of $[H_3N(CH_2)_{17}CH_3]^+$–montmorillonite (CWC) is shown in Figure 4. The distance between the layers is in the range of 40–50 Å. The delamination of clay in the polymerized epoxy resin was confirmed by the absence of *d*001 reflections in the XRD patterns and TEM images.

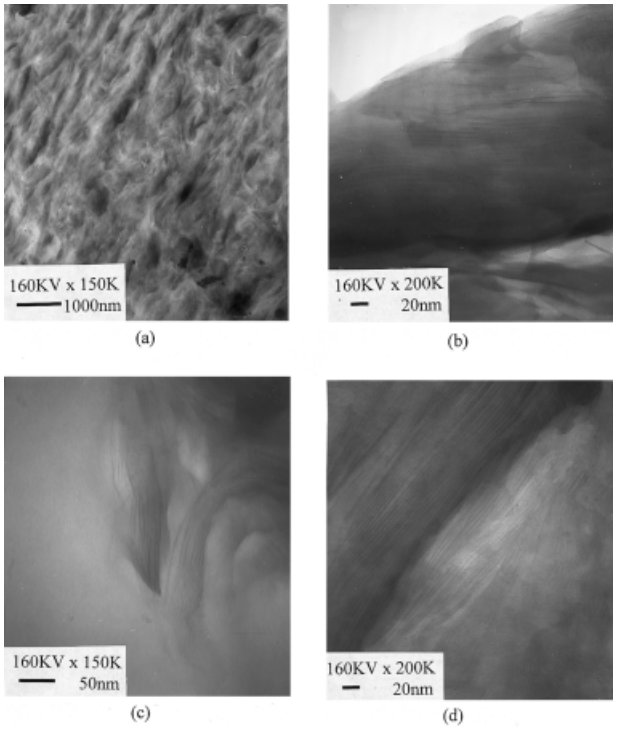

Figure 4 TEM photograph of a clay–epoxy nanocomposite with a $[H_3N(CH_2)_{17}CH_3]^+$–montmorillonite (CWC) content of 20 phr.

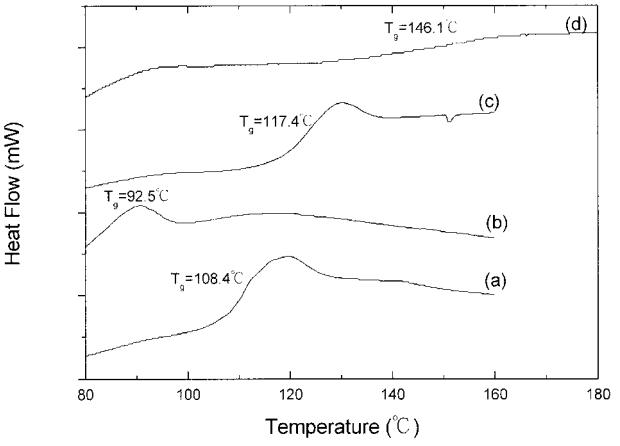

Figure 5 DSC thermograms. Hybrids of clay with (a) no clay addition, (b) 20 phr pristine–montmorillonite (CWC), (c) 5 phr $[H_3N(CH_2)_{17}CH_3]^+$–montmorillonite (CWC), and (d) 20 phr $[H_3N(CH_2)_{17}CH_3]^+$–montmorillonite (CWC).

Properties of the nanocomposite

Several important properties of the nanocomposite were studied. The glass transition temperature (T_g) of the clay–epoxy nanocomposite was determined by DSC. As shown in Figure 5, the epoxy polymer without the addition of clay shows the T_g at 108.4°C. The addition of Na^+–montmorillonite during the polymerization of the epoxy polymer decreased the T_g to 92.5°C. The epoxy resins polymerized in the presence of 5 and 20 phr of $[H_3N(CH_2)_{17}CH_3]^+$–montmorillonite (CWC) show higher T_g's at 117.4 and 146.1°C. The epoxy was to be used as building blocks for PCBs, plastic IC packages, etc., in the computer industry. Thus, water resistance, especially at various clay loadings, is an important characteristic of these materials.

Figure 6 shows the water content of pristine clay (Na^+–montmorillonite) and modified clay {$[H_3N(CH_2)_{17}CH_3]^+$–montmorillonite} in water at 23°C for 24 h. Ep-

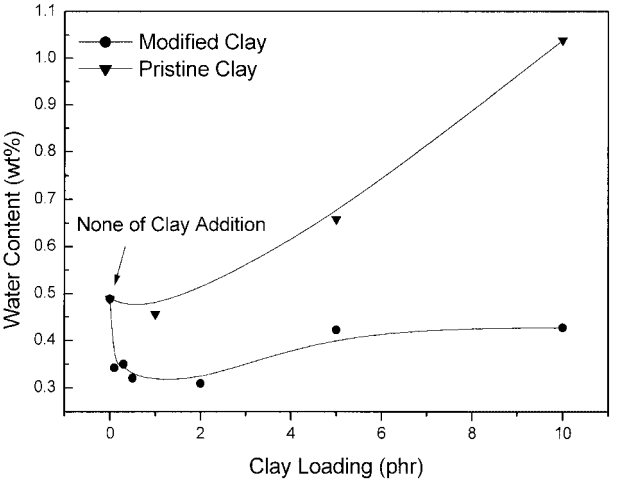

Figure 6 Water content of pristine and modified clay by various clay loadings.

oxy–$[H_3N(CH_2)_{17}CH_3]^+$–montmorillonite nanocomposites show excellent water resistance. The difference of water resistance between modified clay and unmodified clay can be explained by that the water resistance was strongly dependent on the delamination of clay within the epoxy resin and modification of the clay surface. The delamination of clay within the epoxy resin increased the diffusion path of water in the epoxy resin: It took more time for water to pass through the epoxy resin. The modification by $[H_3N(CH_2)_{17}CH_3]^+$ made the clay surface more hydrophobic, because the tail of the onium ions were a hydrophobic group $[CH_3(CH_2)—]$. TGA analyses were also evidence for the affinity of water by the clay surface. Generally, weight loss below 200°C is attributed to desorption of water, which includes interparticle water and interlayer water. The associated weight loss evident in the TGA analysis curve shown in Figure 7 indicates that modification of clay by onium ions such as $[H_3N(CH_2)_{17}CH_3]^+$ was more hydrophobic than was that of unmodified clay.

In this study, the composites are in nanoscale, so they should have better optical properties than just a physical mixture of clay and epoxy resin. Figure 8 shows the transmittance of visible light at 550 nm for modified clay and pristine clay within the epoxy resin. The higher transmittance (% T) of the composite indicates that the clay layers are exfoliated (nanoscale) within the epoxy resin. The epoxy resin with modified clay showed good heat resistance (T_g), water resistance, and optical properties compared with the epoxy resin with no addition of clay or unmodified clay. The results indicate that a nanocomposite of polymer and clay was formed. Unfortunately, epoxy with modified clay resulted in a decrease of tensile strength (not shown here). It is distinct that the interactions between the epoxy and the clay surface are very weak. The mechanism of interaction occurring at the epoxy–clay interface is very complex. Further study about this subject is in progress.

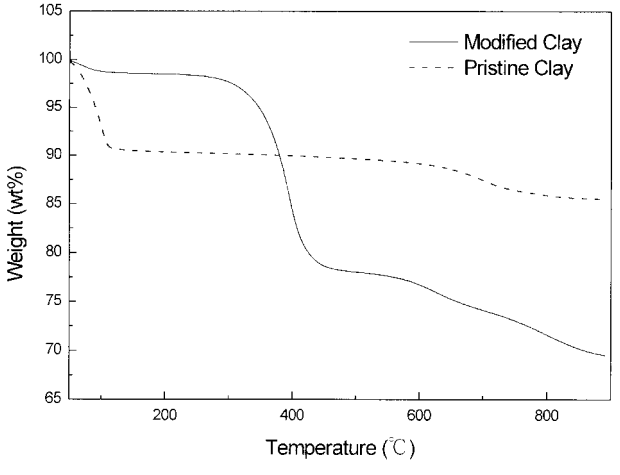

Figure 7 TGA analysis of pristine and modified clay.

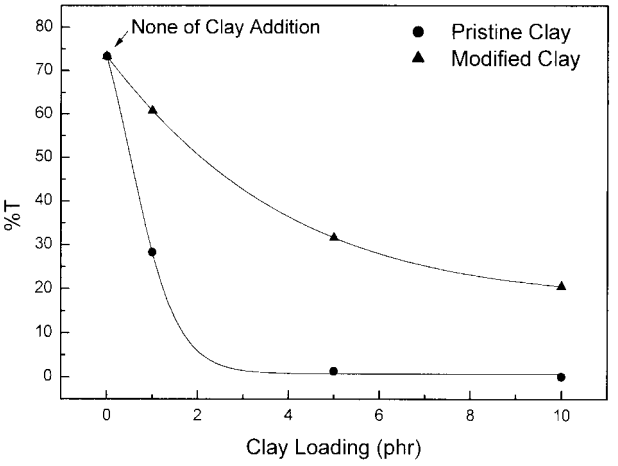

Figure 8 Transmittance of visible light at 550 nm for modified clay and pristine clay within epoxy resin.

CONCLUSIONS

In summary, we attempted to enlarge the *d*-spacing of clay by organic cations. XRD results indicated that the chain length of organic ions play an important role in the *d*-spacing of hybrids. We obtained large *d*-spacing of hybrids when the organic ions had a long chain length. However, due to the charge density of $[H_3N(CH_2)_nNH_3]^{2+}$, the $[H_3N(CH_2)_nNH_3]^{2+}$–clay has smaller *d*-spacing than that of $[H_3N(CH_2)_{n-1}CH_3]^+$–clay or of $[H_3N(CH_2)_{n-1}COOH]^+$–clay. A maximum amount of intercalated cations and *d*-spacing of the intercalated clay were obtained by ion exchange with montmorillonite (CWC). Under the ion-exchanged method, the intercalation of $[H_3N(CH_2)_{11}CH_3]^+$ in the galleries was more efficient than were acid–base methods. The H^+ ions in the galleries may have a little pinning behavior, and the organic ions hardly penetrate the gallery region of the clay. Finally, an clay–epoxy nanocomposite was synthesized successfully with $[H_3N(CH_2)_{17}CH_3]^+$–montmorillonite (CWC). The nanocomposite has good thermal properties, water resistance, and optical properties. The results indicate that a nanocomposite of polymer and clay was formed.

The authors are grateful to Misses S. J. Weng and R. M. Hung of the Precision Instrument Center at the National Central University for their cooperation in the XRD, DSC, ICP–AES, TGA, and TEM studies. The authors also thank Dr. T. Y. Tsai of the Industrial Technology Research Institute in providing the source clay and for valuable discussions.

References

1. Faguy, P. W.; Ma, W. L.; Lowe, J. A.; Pan, W. P.; Brown, T. J Mater Chem 1994, 4, 771.
2. Okada, A.; Kamigaito, O.; Kawasumi, M.; Kurauchi, T. Abstr Pap Am Chem Soc 1987, 194, 10.

3. Usuki, A.; Kojima, Y.; Kawasumi, M.; Okada, A.; Kurauchi, T. Abstr Pap Am Chem Soc 1990, 200, 218.
4. Moet, A. S.; Akelah, A. Mater Lett 1993, 18, 797.
5. Wang, M. S.; Pinnavaia, T. J. Chem Mater 1994, 6, 468.
6. Lan, T.; Pinnavaia, T. J. Chem Mater 1994, 6, 2216.
7. Lan, T.; Kaviratna, P. D.; Pinnavaia, T. J. Chem Mater 1995, 7, 2144.
8. Wu, J. H.; Lerner, M. M. Chem Mater 1993, 5, 835.
9. Lemmon, J. P.; Lerner, M. M. Solid State Commun 1995, 94, 533.
10. Lemmon, J. P.; Wu, J. H.; Oriakhi, C.; Lerner, M. M. Electrochim Acta 1995, 40, 2245.
11. Yano, K.; Usuki, A.; Okada, A. J Polym Sci Part A Polym Chem 1997, 35, 2289.
12. Messersmith, P. B.; Giannelis, E. P. Chem Mater 1993, 5, 1064.
13. Lan, T.; Kaviratna, D.; Pinnavaia, T. J. J Phys Chem Solids 1996, 57, 1005.
14. Pinnavaia, T. J.; Lan, T.; Kaviratna, P. D. ACS Symposium Series 622; American Chemical Society: Washington, DC, 1996; p 250.
15. Burnside, S. D.; Wang, H. C.; Giannelis, E. P. Chem Mater 1999, 11, 1055.
16. Wang, Z.; Lan, T.; Pinnavaia, T. J. Chem Mater 1996, 8, 2200.
17. Wang, Z.; Pinnavaia, T. J. Chem Mater 1998, 10, 1820.
18. Vaia, R. A.; Teukolsky, R. K.; Giannelis, E. P. Chem Mater 1994, 6, 1017.
19. Chen, X. B.; Wu, X. S. Polymer 1992, 33, 3639.
20. Lee, D. C.; Jang, L. W. J Appl Polym Sci 1998, 68, 1997.
21. Lee, A.; Lichtenhan, J. D. J Appl Polym Sci 1999, 73, 1993.
22. Shi, H. Z.; Lan, T.; Pinnavaia, T. J. Chem Mater 1996, 8, 1584.
23. Lagaly, G. Solid State Ionics 1986, 22, 43.